

Supporting Information for

Electronic Resonant Stimulated Raman Scattering Micro-Spectroscopy

Lixue Shi, Hanqing Xiong, Yihui Shen, Rong Long, Lu Wei and Wei Min*

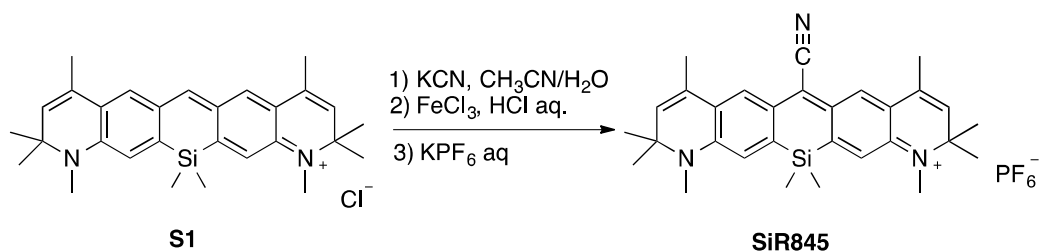
Department of Chemistry, Columbia University, New York, NY 10027, USA

*Correspondence: wm2256@columbia.edu

S1. Synthesis of SiR845

General Methods. Reagents and solvents were purchased from Sigma-Aldrich at the highest commercial quality and used without further purification, unless otherwise stated. All reactions were carried out under a nitrogen atmosphere with dry solvents under anhydrous conditions, unless otherwise noted. Reactions were monitored by thin-layer chromatography (TLC) carried out on glass backed silica gel TLC plates (250 μm) from Silicycle; visualization by UV light, an ethanolic solution of phosphomolybdic acid as staining agent. NMR spectra were recorded on either a Brüker Advance 400 (^1H : 400 MHz, ^{13}C : 100 MHz). Brüker Advance 500 (^1H : 500 MHz, ^{13}C : 125 MHz). High resolution mass spectrometric (HRMS) data were obtained using JMS-HX110A mass spectrometer. The following abbreviations were used to explain the multiplicities: s = singlet, d = doublet, t = triplet, q = quartet, m = multiplet, b = broad.

Synthesis of SiR845:



Synthesis of **S1** follows the same procedures as reported in *J. Am. Chem. Soc.* 2012, 134, 5029-5031. To a solution of **S1** (6.0 mg, 12.6 μmol) in 5 mL acetonitrile and 1 mL water was added KCN solution in H_2O (0.1 M, 250 μL , 25 μmol). The solution was stirred for 30 min before FeCl_3 solution in $\text{HCl}/\text{H}_2\text{O}$ (0.5 M in 1 N HCl, 100 μL , 50 μmol) was added. The solution was stirred for another 1 h before 2 mL 5% KPF_6 aq. solution was added. Then the system was extracted with 3×3 mL DCM. The organic layers were combined, dried over Na_2SO_4 before the solvent was removed *in vacuo*. The product was purified via neutral aluminum oxide flash chromatography (DCM to DCM/MeOH = 9/1) to yield pure **SiR845** (1.3 mg, 2.14 μmol , 17%).

^1H NMR (400 MHz, CD_3OD) δ ppm: 7.75 (s, 2H), 7.28 (s, 2H), 5.77 (d, $J = 1.4$ Hz, 2H), 3.40 (s, 6H), 2.09 (d, $J = 1.4$ Hz, 6H), 1.57 (s, 12H), 0.57 (s, 6H)

HRMS (ESI+) m/z Calcd. for $\text{C}_{30}\text{H}_{36}\text{N}_3\text{Si}^+ [\text{M}]^+$: 466.2679. Found: 466.2682

Supporting Figure S1

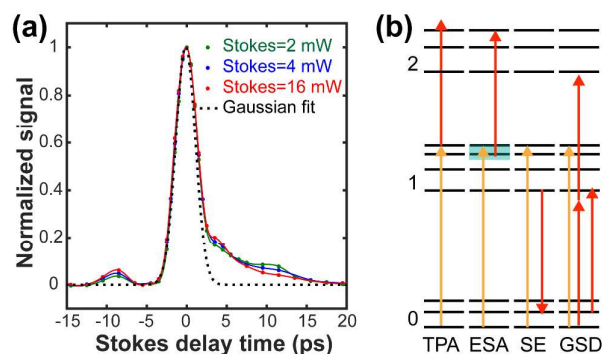


Figure S1. Electronic background is from competing pump-probe processes. (a) Unsymmetrical time delay dependence of the background under different power combinations. Pump was fixed at 4 mW. (b) Energy diagram of possible pump-probe processes.

Supporting Figure S2

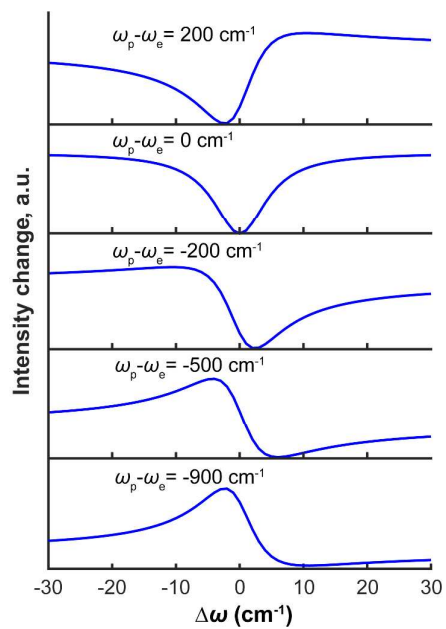


Figure S2. Simulations of er-SRS band shapes using eq 1. $\Delta\omega = \omega_R - (\omega_p - \omega_e)$.

$\Gamma_e = 430$ cm⁻¹, $\Gamma_R = 5$ cm⁻¹ and excitation condition $(\omega_p - \omega_e)$ was indicated inside figure.

Supporting Figure S3-S5

Study of power dependence and saturation effect:

Figure S3-S5 illustrate the power dependence and saturation effect on SiR845, IR820 and IR895, respectively. Taking SiR845 as an example (**Figure S3**). Firstly, for pump power dependence, pump-beam excited fluorescence was first measured to confirm no nonlinear absorption happened for the pump beam. As a result, **Figure S3a** and **Figure S3c** present good linear correlation at pump wavelength either for C=C mode (1609 cm^{-1}) or C \equiv N modes using laser power below $100\ \mu\text{W}$. For er-SRS signal, during this pump power region ($P_{\text{pump}} < 100\ \mu\text{W}$), it presents relatively earlier saturation effect starting at $P_{\text{pump}} \approx 20\ \mu\text{W}$ under relative low Stokes power ($P_{\text{Stokes}} \approx 4\ \text{mW}$) (**Figures S3b** and **Figure S3d**). er-SRS signals were all calculated as the subtraction of ‘Raman resonance on’ and ‘Raman resonance off’ (by tuning the pump wavelength 2-3 nm away from the Raman peak position). Secondly, Stokes power dependence was then determined at 20-30 μW pump power. For Stokes power dependence, er-SRS first presents linear power dependence then starts to saturate after $P_{\text{Stokes}} > 5\ \text{mW}$ (**Figure S3e-h**). In addition, Stokes-beam excited fluorescence was also measured which is mainly from two-photon excitation for SiR845 and presents similar saturation trend as er-SRS (**Figure S3i**). This indicates the existence of ground-state depletion effect caused by competed Stokes one-photon and two-photon absorption. This result explains the Stokes power saturation of er-SRS. Similar saturation effects on either pump or Stokes beams were observed for IR820 (**Figure S4**) and IR895 (**Figure S5**).

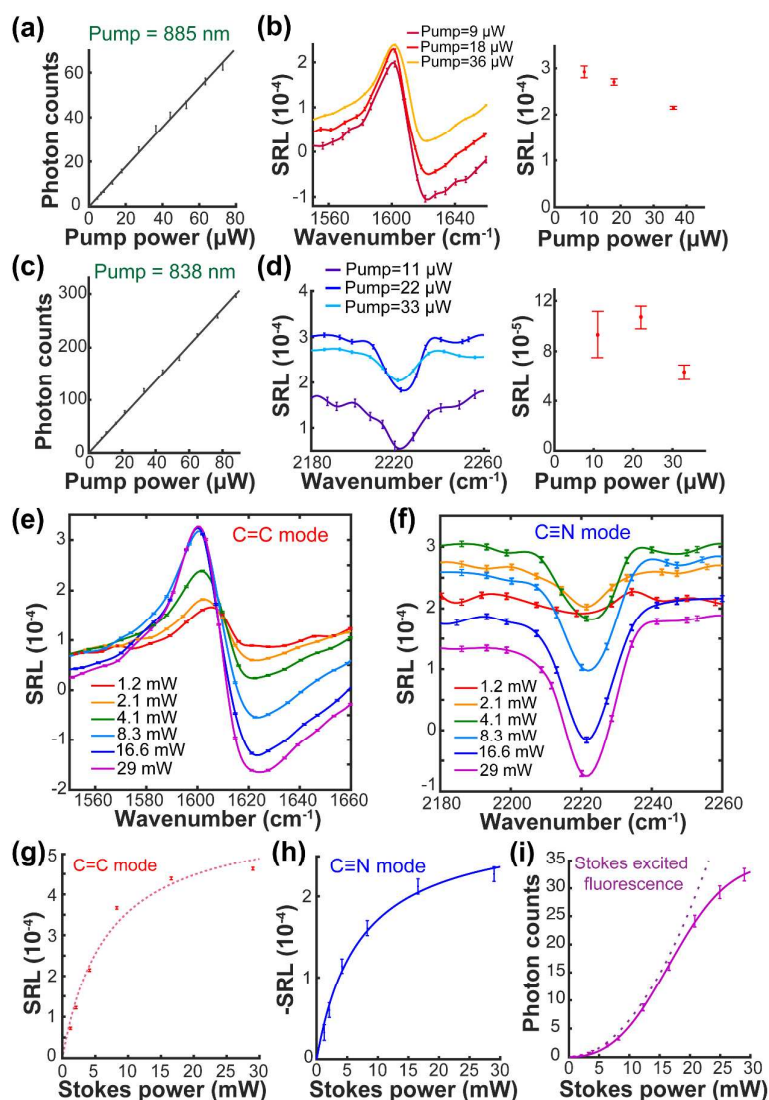


Figure S3. Power dependence study for SiR845. (a-b) SiR845 C=C mode (1609 cm^{-1}) pump power dependence of (a) pump-excited fluorescence (pump set at 885 nm) and (b) er-SRS ($P_{\text{Stokes}}=4.1\text{ mW}$). (c-d) C≡N mode pump power dependence of (c) pump-excited fluorescence (pump set at 838 nm) and (d) er-SRS ($P_{\text{Stokes}}=4.1\text{ mW}$). (e) er-SRS spectra of a C=C mode under different Stokes powers. (f) er-SRS spectra of C≡N mode under different Stokes powers. (g) Stokes power dependence of the C=C mode plotted from measurements in (e). Curve was fitted by a two-level one-photon excitation model. (h) Stokes power dependence of the C≡N mode plotted from measurements in (f). Curve was fitted by a two-level one-photon excitation model. (i) Power dependence curve for Stokes-excited fluorescence presents similar saturation trend as er-SRS process shown in (g-h). Solid line is the fitting of all data points with a two-level two-photon excitation model; dot line is the fitting of low power data (first 5 data points) with the quadratic correlation.

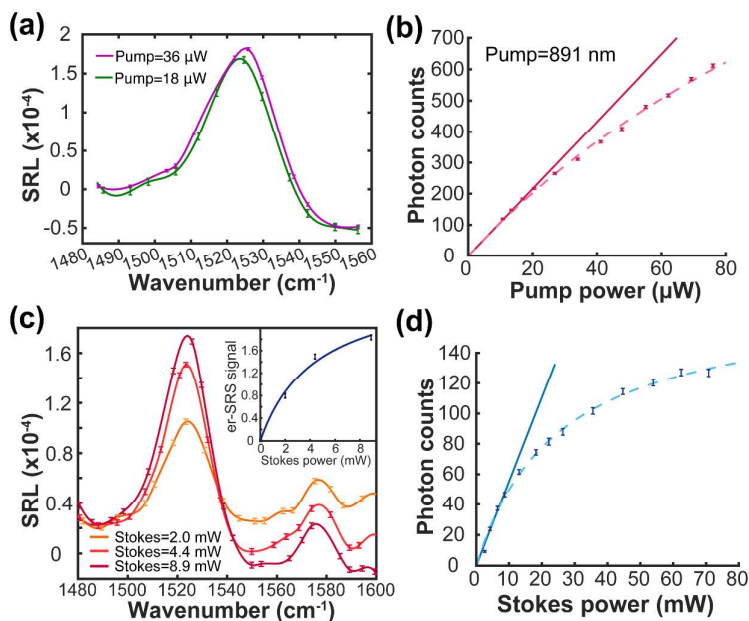


Figure S4. Pump and Stokes power dependence of C=C mode (1526 cm^{-1}) of IR820. (a) er-SRS spectrum under low pump power shows no saturation effect as the SRL are almost the same for two pump power conditions. (b) Liner power dependence for pump-excited fluorescence (pump set at 891 nm) shows no nonlinear absorption happened for pump beam with $P_{\text{pump}} < 20 \text{ } \mu\text{W}$. (c) Stokes power saturation effect on er-SRS signal. $P_{\text{pump}} = 18 \text{ } \mu\text{W}$. (d) Stokes-excited fluorescence also presents saturation trend indicates the existence of ground-state depletion caused by Stokes one-photon absorption. In (b) and (d), solid lines are the fittings of low power data (first 4 data points) with the linear correlation; dashed lines are the fittings of all data points with a two-level one-photon excitation model.

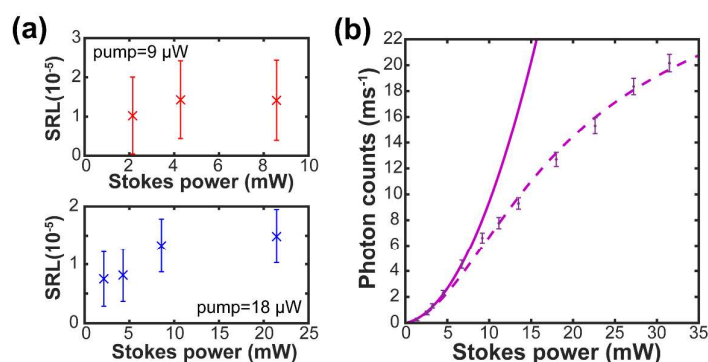


Figure S5. Pump and Stokes power dependence of C=C mode (1576 cm^{-1}) of IR895. (a) current pump and Stokes power already saturate the er-SRS. Lower laser power is prevented by the laser noise and low solubility of IR895. (b) Quadratic power dependence for Stokes-excited fluorescence shows saturation trend after $P_{\text{Stokes}} > 7 \text{ mW}$. Solid line is the fitting of low power data (first 5 data points) with the quadratic correlation; dashed line is the fitting of all data points with a two-level two-photon excitation model.

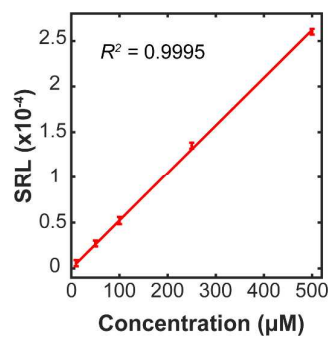


Figure S6. Concentration curve of IR820 solution. Linear concentration curve for 1526 cm^{-1} peak of IR820. The detection limit is $5\ \mu\text{M}$ for $\text{SNR}=1$ under 1-ms time constant. Pump power is about $25\ \mu\text{W}$ and Stokes power is 50 mW.